ADVANCED MATERIALS

Supporting Information

for *Adv. Mater.,* DOI: 10.1002/adma.202109376

Modulating Tumor Extracellular Matrix by Simultaneous Inhibition of Two Cancer Cell Receptors

*Weizhi Chen, Yang Yuan, Cheng Li, Hui Mao, Baorui Liu, and Xiqun Jiang**

WILEY-VCH

Supporting Information

Modulating Tumor Extracellular Matrix by Simultaneous Inhibition of Two Cancer Cell Receptors

*Weizhi Chen, Yang Yuan, Cheng Li, Hui Mao, Baorui Liu, Xiqun Jiang**

W. Chen, Y. Yuan, C. Li, X. Jiang
College of Chemistry and Chemical Engineering
Nanjing University, Nanjing 210023, China
E-mail: jiangx@nju.edu.cn.

H. Mao
Department of Radiology and Imaging Sciences
Emory University, Atlanta GA 30322, USA

B. Liu
The Comprehensive Cancer Centre of Drum Tower Hospital
Medical School of Nanjing University, Nanjing 210008, China

Experimental Section

Expression and purification of RPs: Standard molecule biology methods were used to construct the recombinant plasmids of RP-R, RP-E and RP-ER from the recombinant plasmid RP reported previously.[1] RP was comprised of VPGXG, where X = K: V: F in a 1:2:1 ratio. The amino acid sequence of RP-ER can be found in Figure S1A. RP, RP-R, RP-E, and RP-ER were expressed from *E. coil* strain BL21 (DE3) in TB media without IPTG induction. RP and RP-R were purified using the inverse transition cycling (ITC) method.[2] RP-E and RP-ER were purified by immobilized metal affinity chromatography (IMAC) using a HisTrp column and a AKTA purify system. All RP, RP-R, RP-E, and RP-ER were dialyzed into 10 mM PBS and stored at 4 ºC for further use.

Synthesis of DOX-hydrazone: The synthesis route of 3-(2-pyridinyldithio) propanoic acid doxorubicin hydrazide (DOX-hydrazone) is shown below. Briefly, three steps are included and the details are shown below.

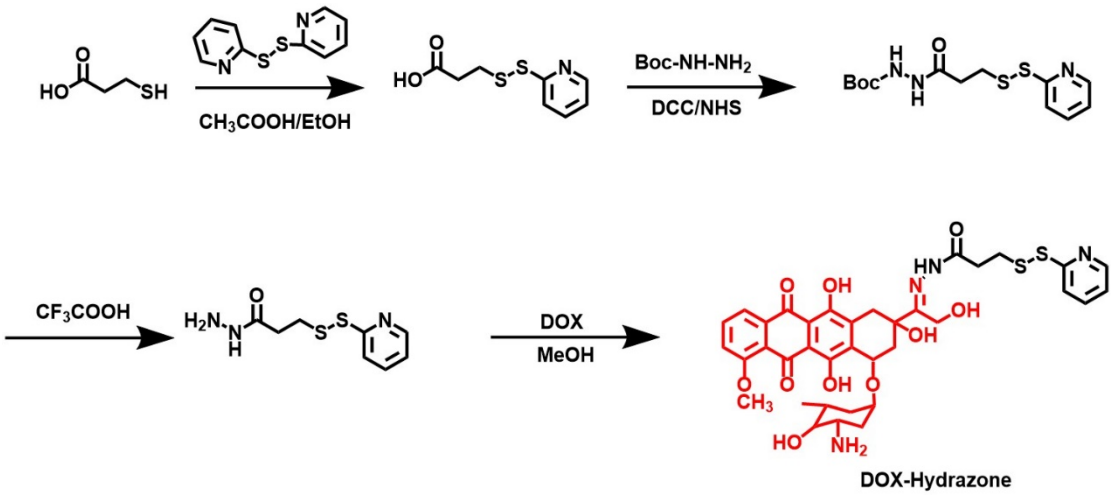

Synthesis of 3-(2-pyridinyldithio) propanoic acid (PDP): 2,2'-Dithiodipyridine (3.75 g) was dissolved in 10 mL ethanol and 0.4 mL of glacial acetic acid was added. The solution was stirred vigorously and then 0.9 g of 3-mercaptopropionic acid in 5 mL of ethanol was added dropwise. The solution was left at room temperature for 20 h. The solvent was then removed by evaporation under reduced pressure to yield a viscous yellow oil. The crude product was purified by a basic Al_2O_3 column using a 3:2 mixture of dichloromethane and ethanol as eluent. Once the yellow band corresponding to the thione by-product had eluted from the column, 4 mL of acetic acid per 100 mL solvent was added to elute the desired product. Fractions containing this compound were pooled and the solvent was removed under reduced pressure.

The resulting product PDP was dried in a vacuum oven and yielded viscous oil. ^{1}H NMR (400 MHz, $CDCl_3$): δ = 2.85 (t, 2H), 3.07 (t, 2H), 7.23 (ddd, 1H), 7.75 (d, 1H), 7.8 (td, 1H), 8.49 (d, 1H).

Synthesis of Boc protective 3-(2-pyridinyldithio) propanoic acid hydrazide: PDP (200 mg) and N-hydroxysuccinimide (NHS) (270 mg) were dissolved in 10 mL anhydrous dichloromethane. Then N, N′-Dicyclohexylcarbodiimide (DCC) (420 mg) in 5 mL anhydrous dichloromethane was added. The solution was stirred at 0 ºC for 10 min and then room temperature for another 3 hours. Tert-butyl carbazate (300 mg) was subsequently added into the solution and followed reaction for another 24 hours. The precipitate was removed by filtration and the solvent was removed by evaporation under reduced pressure. The resultant crude product was then purified by silica gel column with a 4:1 mixture of n-hexane and ethyl acetate as eluent. Then the solvent was removed by rotary evaporation and yielded a white solid. ^{1}H NMR (400 MHz, $CDCl_3$): δ = 10.98 (s, 1H), 10.12-10.54 (s, 2H), 8.49- 7.14 (m, 4H), 1.47(s, 9H), 2.7 (t, 2H), 3.07 (t, 2H), 6.78 (d, 1H),7.23 (ddd, 1H), 7.75 (d, 1H), 7.8 (td, 1H), 8.49 (d, 1H), 9.3 (s, 1H).

After the deprotection of Boc group, it resulted in 3-(2-pyridinyldithio) propanoic acid hydrazide. Briefly, 100 mg Boc protective 3-(2-pyridinyldithio) propanoic acid hydrazide was dissolved in 5 mL dichloromethane and then 5 mL trifluoroacetic acid (TFA) 1:1. The mixture was stirred for 24 hours and the solvent was removed by rotary evaporation. The resultant 3-(2-pyridinyldithio) propanoic acid hydrazide was precipitated with diethyl ether three times and then dried at high vacuum. ^{1}H NMR (400 MHz, DMSO-d6): δ = 2.7 (t, 2H), 3.07 (t, 2H), 6.78 (d, 1H),7.23 (ddd, 1H), 7.75 (m, 2H), 7.8 (td, 1H), 8.4 (td, 1H).

Synthesis of DOX-Hydrazone: DOX-hydrazone was synthesized as described previously.[3] Briefly, adriamycin hydrochloride (25 mg, 0.043 mmol) was stirred in anhydrous methanol (375 mL) and treated with 3-(2-pyridinyldithio) propanoic acid hydrazide (13.4 mg, 0.0585 mmol) followed by one drop of TFA. After stirring overnight at room temperature, a clear solution was obtained. The solvent was evaporated; the residue was re-dissolved in anhydrous methanol (0.5 mL). The methanolic solution was added dropwise to stirred acetonitrile (30 mL) to precipitate the desired product. The solid obtained was collected by centrifugation and dried at high vacuum. HPLC was used to monitor the interaction process and analysis of the purity of the product. CH_3OH-50 mM (NH_4) (H_2PO_4) (7:3) was used as a mobile phase. And the retention times of free DOX, free hydrazide and DOX-hydrazone detected by UV (280 nm) were 3.2 min, 4.0 min, and 5.0 min, respectively.

Synthesis of RPDCs: DOX-hydrazone was conjugated with recombinant proteins through a two-step reaction. First, 2 mg mL^{-1} of different recombinant proteins (RPs) was reacted with a predetermined amount of NHS-PEG-MAL (1000 Da, Ponsure Biotechnology) in 0.1 M phosphate buffer (pH 6.5) at 4 °C for 8 h. The unreacted PEG was separated by ultrafiltration. DOX-hydrazone was then conjugated with proteins through the click chemistry based on the reaction between sulfydryl and MAL in the presence of 20 mM tris(2-carbox-yethyl) phosphine. Free DOX-hydrazone was further removed through gel filtration chromatography with a G-25 gel column. The purified RPDC, RPDC-R, RPDC-E and RPDC-ER were then concentrated by ultrafiltration.

Characterization of RPs and RPDCs: The purity and molecular weights of RPs were identified by 12% sodium dodecyl sulfate polyacrylamide gel electrophoresis (SDS-PAGE) and further analyzed by matrix-assisted laser desorption/ionization time of flight mass spectroscopy (MALDI-TOF-MS). The concentrations of RPs were calculated by the molar extinction coefficient at 280 nm based on their primary amino acid. The zeta potentials of RPs before and after drug conjugation were measured using a Brookhaven BI9000AT system (Brookhaven Instruments Corporation, USA). The secondary structures of RPs were analyzed by circular dichroism (CD) spectrum from 190 nm to 250 nm using a MOS-500 CD spectrometer (Bio-Logic Science Instruments, France). The hydrodynamic diameters of RPDCs were measured by dynamic light scattering (DLS) in 10 mM PBS. The absorption spectrum of free DOX and four RPDCs were measured by a UV-Vis spectrophotometry in 10 mM PBS, respectively. The drug content (DC) of RPDCs were calculated from MALDI-TOF-MS data using the following formula: $DC = W_{DOX}/W_{protein}$.

Measurements of drug release: 0.1 M sodium acetate buffer (pH 5.3) and 0.1 M phosphate buffered saline (pH 6.5 and 7.4) were used as the release medium. The DOX concentration of the release medium was determined by the fluorescence intensity of DOX and measured using a fluorescence spectrometer (RF-5301PC, Shimadzu, Japan) at an excitation wavelength of 480 nm and an emission wavelength of 590 nm and referenced to a calibration curve.

Cell culture: The cell lines HeLa, MCF-7 and NIH3T3 were purchased from the American Type Culture Collection (ATCC). A549 and MIA PaCa-2 cells were obtained from Procell Life Science &Technology Co, Ltd. MDA-MB 231 cells were provided by the drum tower hospital

of Nanjing University. HeLa, MCF-7, MDA-MB 231 and NIH3T3 cells were cultured in DMEM medium (Gibco) supplemented with 10% FBS (Wisent). A549 cells were cultured in F12K medium (Procell). All medium were supplemented with 1% penicillin/streptomycin (Gibco). Cells were grown in a humidified incubator (Heal Force) with 5% CO_2 at 37 ºC.

Measurements of cytotoxicity and cellular uptake: HeLa cells were used to measure the cytotoxicity and cellular uptake of different RPDCs by a standard 3-(4,5-dimethylthiazol-2-yl)-2,5-diphenyltetrazolium bromide (MTT) assay. The cytocompatibilities of four recombinant proteins were also tested using mouse embryo fibroblast NIH3T3 cells. The cellular uptakes of rhodamine B (RB)-labeled recombinant proteins were observed by confocal laser scanning microscopy (CLSM; LSM 710, ZEISS, Germany) through an x63 oil immersion lens. For the competition or blocking experiment, cetuximab (25 μg mL^{-1}) was co-incubated with RB-labeled RP-ER in HeLa cells. For flow cytometry analysis, cells were digested with trypsin to a single cell suspension and then analyzed using a flow cytometer (Accuri C6, BD Biosciences, USA).

Endocytosis pathway analysis: To further evaluate the endocytosis pathways of RPDCs in HeLa cells, the endocytosis inhibitors were added 1 hour before cells treated with PRDC, RPDC-R, RPDC-E, and RPDC-ER for 2 h in 37 ºC. Chlorpromazine (CPZ) (10 μM), Methyl-β-cyclodextrin (MβCD) (300 μM), 5-(N-ethyl-N-isopropyl) amiloride (EIPA) (100 μM) which are used as inhibitors of clathrin-mediated endocytosis, caveolae-mediated endocytosis, and micropinocytosis. After incubation, the cells were rinsed with PBS for three times and trypsinization. After removing trypsin by centrifugation, the cells were collected and analyzed by a flow cytometer (Accuri C6, BD Biosciences, USA).

Measurement of transcellular transportation: For transcellular transportation experiments, HeLa cells were seeded on coverslips and incubated overnight. The cells on the first coverslip were first cultured with different RPDCs (10 μg mL^{-1} for DOX concentration) for 6 hours. The cells on the first coverslips were rinsed with PBS and then co-incubated with fresh cells on the second coverslips in a fresh medium for 12 hours. The cells on the second coverslips were then taken out and rinsed, followed by culturing fresh cells on the third coverslips in a fresh culture medium for another 24 hours. Finally, the cells were rinsed and stained for nuclei with Hoechst 33258 before imaging by CLSM. To evaluate the transcellular transportation delivery efficacy of RPDC-ER in HeLa cells, the medium and cells in each round were collected at the end of

the transcellular delivery experiment. The DOX in these samples were extracted by the extract solution (70% ethanol with 0.3 N HCl). The DOX concentrations were eventually quantified using a fluorescence spectrometer at an excitation/emission wavelength of 480 and 590 nm. The transcellular transportation efficacy of RPDC-ER was calculated by the ratio of the DOX contents transferred to the next round to the total DOX contents in the cells in the prior round.

Western blots: Western blots were performed following standard protocols. Protein lysates from cancer cells were prepared using RIPA buffer, separated by gel electrophoresis and transferred to polyvinylidene difluoride membranes. After incubated with the block solution (5% skim milk powder in TBST) for 1 hour at room temperature, the membranes were incubated with primary antibodies at 4 °C overnight, followed by incubation with the HRP-conjugated goat anti-rabbit secondary antibody (Proteintech, SA00001-2, USA) at room temperature for 1 h. Proteins on the membranes were imaged using a Electro-Chemi-Luminescence (ECL) instrument (Tanon-5200, Tanon Science & Technology Co., Ltd. Shanghai, China). Primary antibodies used were anti-EGFR (Cell Signaling Technology, 4267, USA), anti-integrin $\alpha_v\beta_3$ (Novus biologicals, NBP2-67557, USA), anti-FAK (Abcam, ab40794, USA) and anti-GAPDH (Proteintech, 10494-1-AP, USA).

qRT-PCR: Total RNA from cancer cells was extracted using TRIzol (Thermo Fisher Scientific) and then reversed transcribed using the PrimeScript™ RT reagent kit (TaKaRa, RR047A) according to the manufacturer's instructions. Quantitative PCR was performed with TB Green *Premix Ex Taq™* II (Tli RNaseH Plus) (TaKaRa, RR820A) on the real-time PCR system (BIOER，FQD-48A). The expression level of mRNA was calculated using the ΔCt method and normalized to *ACTB*.

Mice: All animal experiments were performed in compliance with guidelines set by the Animal Ethical and Welfare Committee at Nanjing University (Nanjing, China) (ID: 2003100). Male and female 6–8-week-old ICR or BALB/c nude mice were purchased from Qinglongshan Animal Breeding Farm. Mice were maintained under specific pathogen-free conditions, and food and water were provided ad libitum. Mice were randomly assigned to the experimental groups.

Histological analysis: Histological and immunofluorescence staining were performed following standard protocols. Tumor tissue samples were fixed in 4% paraformaldehyde at 4

°C for 4 h, dehydrated with 25% sucrose solution overnight and cut into 9-μm sections by a freezing microtome (Lecia). Primary antibodies used were anti-collagen I (Abcam, ab21286, USA), anti-αSMA (Abcam, ab32575, USA) and anti-TGFβ1 (Proteintech, 21898-1-AP). Alexa 488 conjugated goat anti-rabbit secondary antibody was from Invitrogen, USA. The cellular nucleus was stained by DAPI. Tumors were fixed in 4% formalin, embedded in paraffin and cut into 9-μm sections. Sections were subjected to hematoxylin and eosin (H&E) staining, Sirius Red staining and Masson staining to detect the expression of collagen I. F-actin was visualized by FITC-labeled phalloidin (Yeasen, 40735ES75).

Measurement of tumor tissue pressures and stiffness: The tumor interstitial fluid pressure was measured by a multi-channel physiological signal acquisition system (Chengdu Instrument Factory, China). For measuring the tumor solid stress, tumors collected from mice were cut through the middle to about 80% along the long axis and immersed into PBS for 5 min. The tumor opening size was measured by a vernier caliper and solid stress was calculated by the ration of the opening size to the diameter that perpendicular to the incision.[4] The tumor stiffness was measured as Young's modulus. The tumors were excised, trimmed and then compressed by a universal material testing machine (Instron3366, Instron, USA) with a speed of 0.5 mm min^{-1} until the breaking point of the testing tissue was reached. The Young's modulus was calculated by the ration of stress to strain from the obtained stress-strain curve recorded by the system.

Proteomic analysis: At 16 hours post-injection, tumors with and without RP-ER treatment were collected, lysed with sonication in the lysis buffer supplemented with 1 mM PMSF. Insolubles were removed by centrifugation. Protein concentrations were determined by BCA assay and aliquoted to store at -80 °C until ready for analysis of the mass spectrometry. In preparation for mass spectrometry, 100 μg proteins were subjected with 120 μL reducing buffer (4.5 mM DTT, 8 M Urea, 100 mM TEAB, pH 8.0) and incubated at 50°C for 1 hour. Samples were then cooled to room temperature and alkylated with 50 mM iodoacetamide solution in the dark for 40 min at room temperature. After the washing step, 100 μL 300 mM TEAB was added and the samples were digested with 3 μg sequencing-grade trypsin (HLS TRY001C) at 37°C overnight. The supernatant was collected by centrifugation and the pHs were adjusted to acidic using H_3PO_4. The digested peptides were desalted by C18-Reverse-Phase SPE Column and then analysed by a Q-Exactive mass spectrometer (Thermo, USA) equipped with a Nanospray Flex source (Thermo, USA). Proteome Discoverer (v.2.3) was used to search all of the Q-Exactive raw data

thoroughly against the sample protein database. The differential protein expressions were used for Gene Ontology (GO) terms and KEGG pathways analysis through DAVID Bioinformatics Resources to understand the underlying molecular mechanism for RP treatment.[5,6]

Measurement of drug distribution in multicellular spheroids (MCs): HeLa MCs were formed similar to SH-SY5Y MCs.[7] Several HeLa MCs were incubated with RPDC, RPDC-R，RPDC-E, RPDC-ER and free DOX (DOX eq.) with or without RP-ER for 8 hours and 16 hours at 37 ºC and then observed by a CLSM (Zeiss LSM710). The mean fluorescence intensity in each MC was measured by the ZEN 2008 program. Migration index (MI), retention index (RI) and distribution index (DI) were defined to quantify the retention and migration capacity of the RPDCs, from those reported by Bahareh Behkam with a little modification.[8] Since we use MCs as a system to simulate the tumors, MCs were scanned by CLSM at the maximum focal plane and each section was segmented into 50 μm thick ring elements located at radial locations of R_i from the surface of the tumor (Figure 5G). MI is a measurement of the intratumoral penetration depth of the therapeutic agents toward the center of the MC or a simulated tumor. It is defined as:

$$MI = \frac{\sum_{i=1}^{N} R_i \cdot N_i}{R_{max} \cdot N}$$

where R_i is the radial location of segment i measured from the tumor surface, N_i is the concentration of the drugs within segment i and is presented as fluorescence intensity of DOX that is correlated to its concentration; R_{max} is the theoretical maximum migration distance (*i.e.*, radius of the tumor spheroid); and N is the total concentration of drugs detected within the whole MCs slice. The MI value ranges from 0 to 1, wherein a value of 1 indicates that all of the drugs traveled to the center of the tumor and 0 indicates that all of the drugs remained at the periphery of the tumor. RI is the concentration density of drugs within a given tumor and is defined as:

$$RI = \frac{N}{S}$$

where S is the area of the entire MCs slice. The value of RI describes the tumor retention of the drug without consideration of its spatial distribution. DI represents a composite normalized index of migration and retention, defined as:

$$DI = \frac{MI \times RI}{(MI \times RI)_{free\ DOX}}$$

where $(MI \times RI)_{free\ DOX}$ represents the intratumoral distribution of free DOX. Thus, the DI provides a relative measurement of intratumoral distribution efficacy compared with free DOX.

Measurements of intratumoral distribution and penetration of RPDCs: FITC labeled dextran (200 kDa) was intravenously injected into HeLa tumor-bearing mice for *in vivo* visulization of the blood vessel. An arc-shaped incision was made around the subcutaneous tumor without damaging the vessels. Mice in assigned groups were treated with different RPDCs with equal DOX concentration (5 mg kg^{-1}) respectively. In order to block EGFR, 2 mg cetuximab (Merck) was i.v. injected 2 hours prior to the RPDC injection. Tumors were imaged using a CLSM (ZEISS LSM710). The FITC and DOX signals were detected using 488/520 and 488/590 nm excitation/emission filters, respectively. The intratumoral distribution of RPDCs was measured based on fluorescence of DOX. Free DOX and different RPDCs with the equal DOX concentration were i.v. injected into mice bearing HeLa tumor. At 16 hours, tumors were harvested, fixed, dehydrated and cut into 9 μm sections. Tumor vessels were stained by an anti-mouse CD31 antibody (BD Biosciences) and Alexa-594 conjugated secondary antibody (Thermo Fisher Scientific, A21209). The sections were imaged using a CLSM (Leica suite X).

Measurement of tissue distribution: Free DOX, RPDC, RPDC-R, RPDC-E and RPDC-ER were injected i.v. into HeLa tumor-bearing mice (5 mg kg^{-1} DOX eq., n = 3 per group). At each predetermined time, mice were sacrificed to collect tissues samples. After the samples were weighed, DOX in tissues were extracted by an extract solution (70% ethanol with 0.3 N HCl). DOX concentrations were measured using a fluorescence spectrometer at an excitation/emission wavelength of 480 and 590 nm. The pharmacokinetic studies of free DOX and four RPDCs were performed in healthy ICR mice. The blood samples were collected at predetermined times from mouse orbits. The DOX content in plasma was quantified by fluorescence spectrum using the same procedures as above.

Assay for measuring the antitumor efficacy: A maximum tolerated dose (MTD) was first determined. Healthy ICR mice with body weight of 18–22 g were randomly divided into nine groups (n = 3 per group). The mice injected with PBS were used as the control. Different doses of free DOX (5 mg kg^{-1}, 10 mg kg^{-1}), RPDC (5 mg kg^{-1}, 10 mg kg^{-1}, 20 mg kg^{-1}, DOX eq.), RPDC-R (5 mg kg^{-1}, 10 mg kg^{-1}, 20 mg kg^{-1}, DOX eq.), RPDC-E (5 mg kg^{-1}, 10 mg kg^{-1}, 20 mg kg^{-1}, DOX eq.) and RPDC-ER (5 mg kg^{-1}, 10 mg kg^{-1}, 20 mg kg^{-1}, DOX eq.) were administered *via* the caudal vein. The body weights of mice in each group were monitored every

day. The anticancer efficacies of RPDCs were evaluated in mice bearing HeLa tumors. Saline was used as the control. The doses determined in the dosage study were 5 mg kg^{-1} (free DOX), 20 mg kg^{-1} (RPDC, DOX eq.), 20 mg kg^{-1} (RPDC-R, DOX eq.), 20 mg kg^{-1} (RPDC-E, DOX eq.) and 20 mg kg^{-1} (RPDC-ER, DOX eq.), respectively. Agents were given to the mice i.v. The tumor size was measured by a vernier caliper every two days. The tumor volume (V) was calculated using the following equation: $V = (ab^2)/2$, where a and b correspond to the longest and shortest diameter of the tumors, respectively. At the end of the experiment, the tumors were collected for H&E and Ki67 staining.

Statistics analysis. Statistical analysis was performed using Graphpad prime software. Unpaired t-test or multiple t-tests was used to determine statistical significance. The sample sizes were showed in the figure legends. Data were presented as mean ± s.d. Differences between data sets were considered significant when $P < 0.05$.

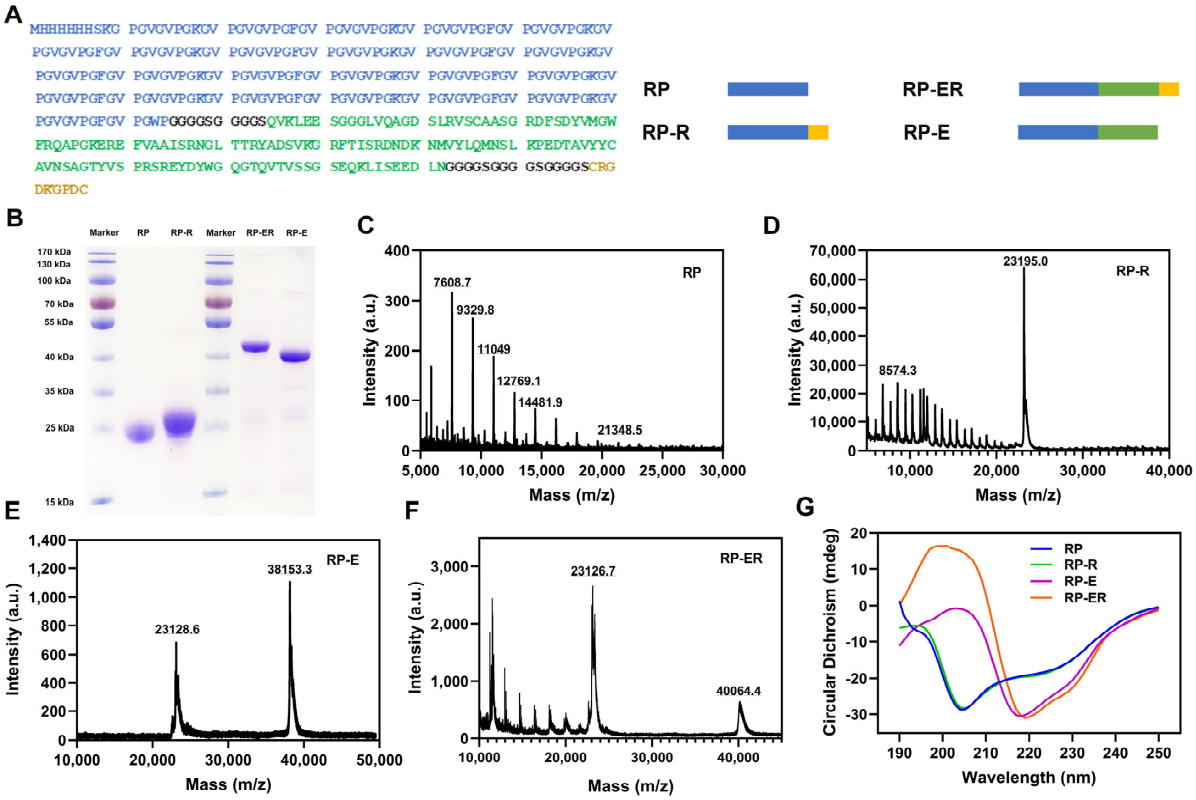

Figure S1. Anti-EGFR nanobody and RGD peptide are linked to RP to make RP-ER. A) The amino acid sequence of RP-ER. RP chain, anti-EGFR nanobody and RGD moiety are colored blue, green and yellow, respectively. The black colored part is the linking spacer. B) The SDS-PAGE of RP, RP-R, RP-ER, and RP-E. C–F) The spectra of matrix-assisted laser desorption/ionization time of flight mass spectroscopy (MALDI-TOF-MS) for RP (C), RP-R (D), RP-E (E) and RP-ER (F), respectively, with sinapic acid as the matrix. G) The circular dichroism (CD) spectra of RP, RP-R, RP-E, and RP-ER in 50 mM NaH_2PO_4 buffer.

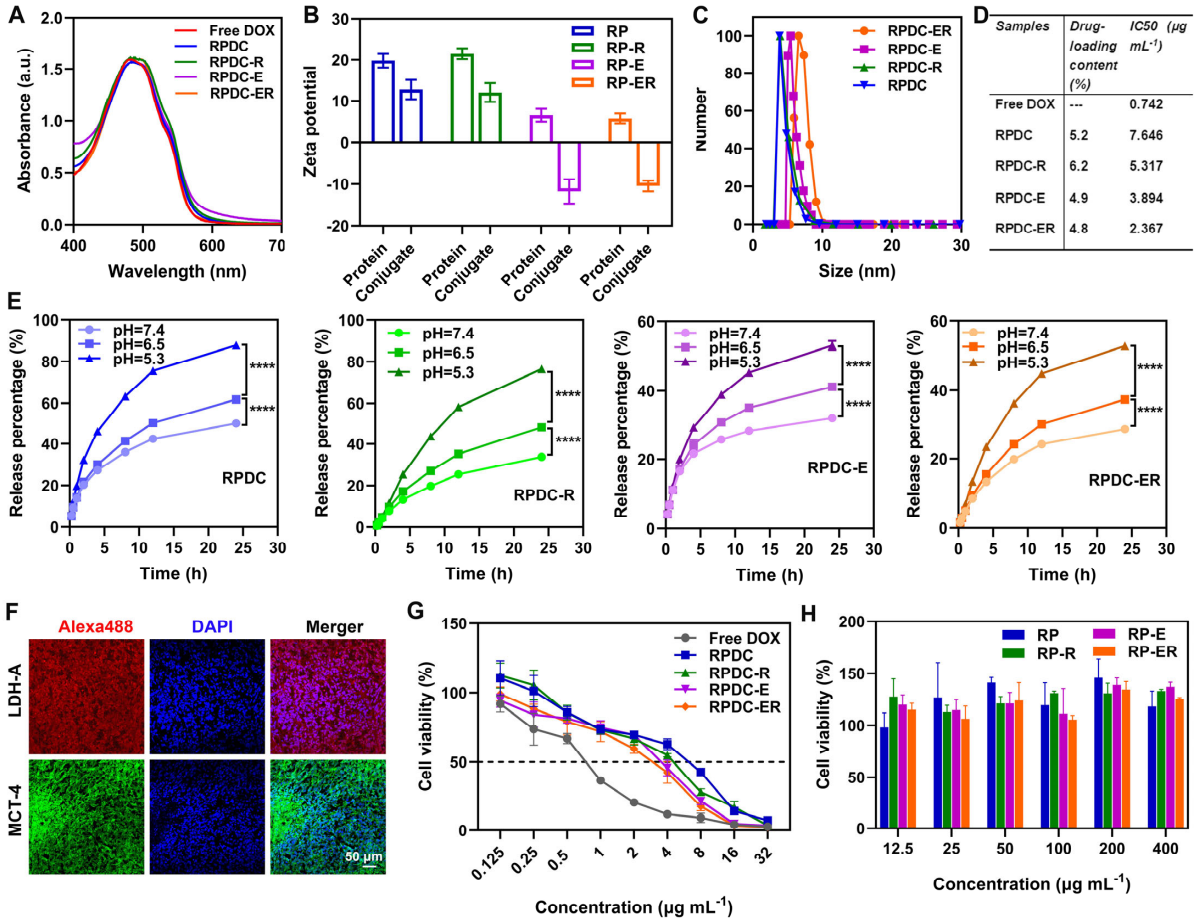

Figure S2. RPs are conjugated with DOX to make RPDCs. A) The UV-Vis absorption spectra of free DOX, RPDC, RPDC-R, RPDC-E and RPDC-ER in 10 mM PBS. B) Zeta potentials of RPs and RPDCs measured in 10 mM PBS. Data are presented in mean ± s.d. (n = 3). C) The hydrodynamic sizes of RPDCs in 10 mM PBS determined by DLS. D) RPDCs have a drug loading content of ~ 5% as calculated from MALDI-TOF. E) RPDCs show acid-labile drug release behaviors. Data are presented in mean ± s.d. (n = 3). P values were calculated using multiple t-tests. **** $P < 0.0001$. F) The acidity-related markers including monocarboxylate transporter 4 (MCT-4) and lactate dehydrogenase A (LDH-A) were upregulated in HeLa tumor tissues. G) RPDCs show a concentration-dependent cytotoxicity against HeLa cells for 24 h (n = 3). Data are presented in mean ± s.d. H) RPs show no cytotoxicity against normal mouse embryo fibroblast NIH3T3 cells when incubated for 24 h (n = 3). Data are presented in mean ± s.d.

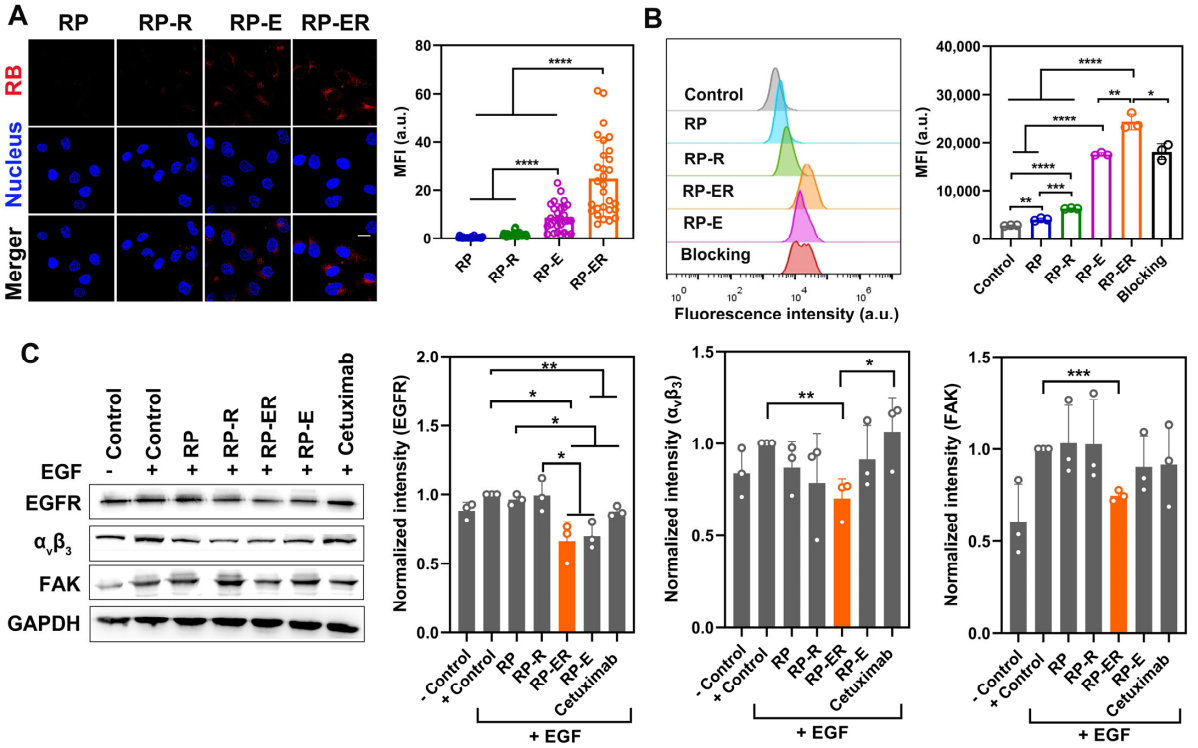

Figure S3. RP-ER reduces the expressions of the ECM biomarkers and exhibits an enhanced cellular internalization ability in cancer cells. A,B) RP-ER shows an enhanced cellular internalization ability determined by CLSM images (A) (n = 29) and flow cytometry analysis (B) (n = 3). C) RP-ER reduces the expression of EGFR, integrin $\alpha_v\beta_3$ and FAK in HeLa cells. The results were determined based on the western blots and quantification of western blots. (n = 3). Data are presented in mean ± s.d. P values were calculated using multiple t-tests. *P < 0.05, ** P < 0.01, *** P < 0.001, **** P < 0.0001.

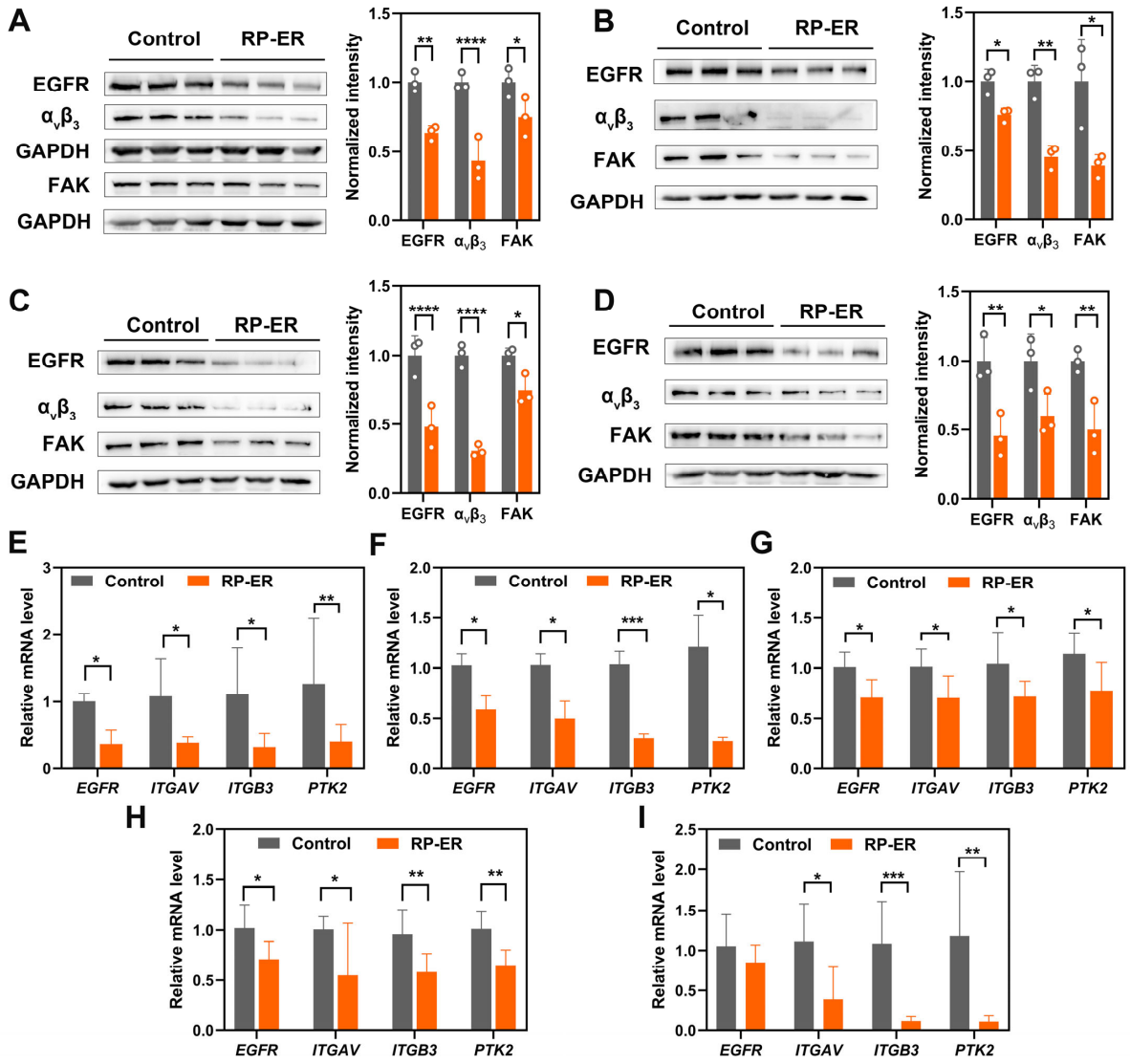

Figure S4. RP-ER reduces the expressions of specific biomarkers in various cancer cells. A–D) RP-ER downregulated the expression of EGFR, integrin $\alpha_v\beta_3$ and FAK in MCF-7 cells (A), MDA-MB 231 cells (B), A549 cells (C) and MIA PaCa-2 cells (D). Intensities in western blots were normalized by ImageJ (n = 3). E–I) RP-ER downregulates the mRNA levels of *EGFR*, *ITGAV*, *ITGB3* and *PTK2* in HeLa cells (E), MCF-7 cells (F), MDA-MB 231 cells (G), A549 cells (H) and MIA-PaCa2 cells (I) (n = 3–7). The data were obtained by qRT-PCR. Data are presented in mean ± s.d. P values were calculated using multiple t-tests. *P < 0.05, ** P < 0.01, *** P < 0.001, **** P < 0.0001.

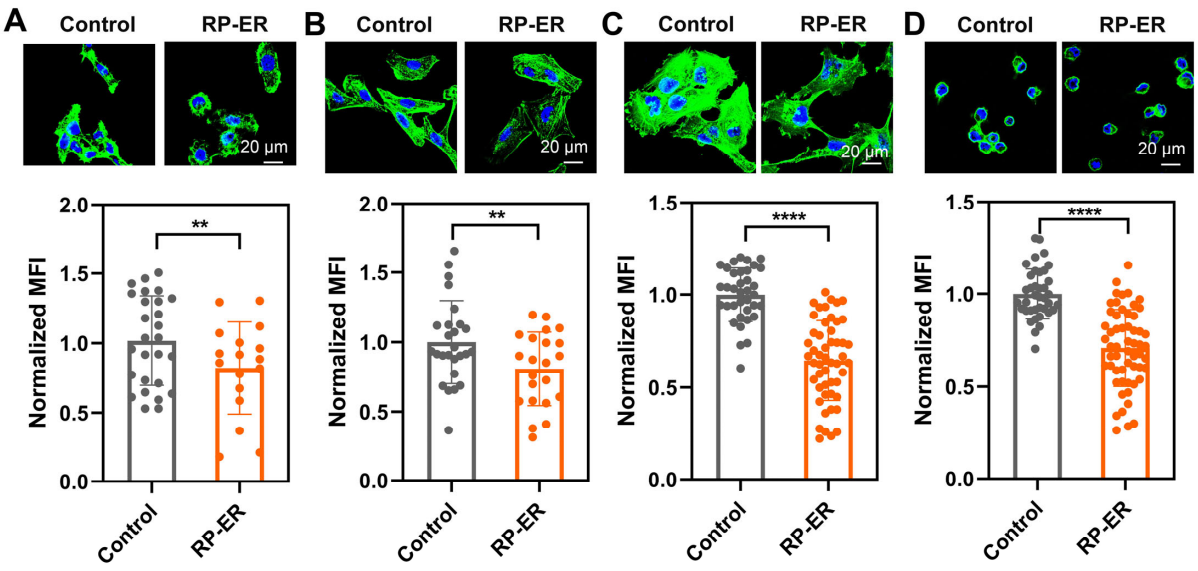

Figure S5. RP-ER reduces the F-actin contents in various cancer cells. The levels of intercellular F-actin in MCF-7 cells (A), A549 cells (B), MDA-MB 231 cells (C) and MIA PaCa-2 cells (D) with or without the treatment of RP-ER were evaluated by FITC-labeled phalloidine. (n = 17–57). Data are presented in mean ± s.d. P values were calculated using multiple t-tests. ** $P < 0.01$, **** $P < 0.0001$.

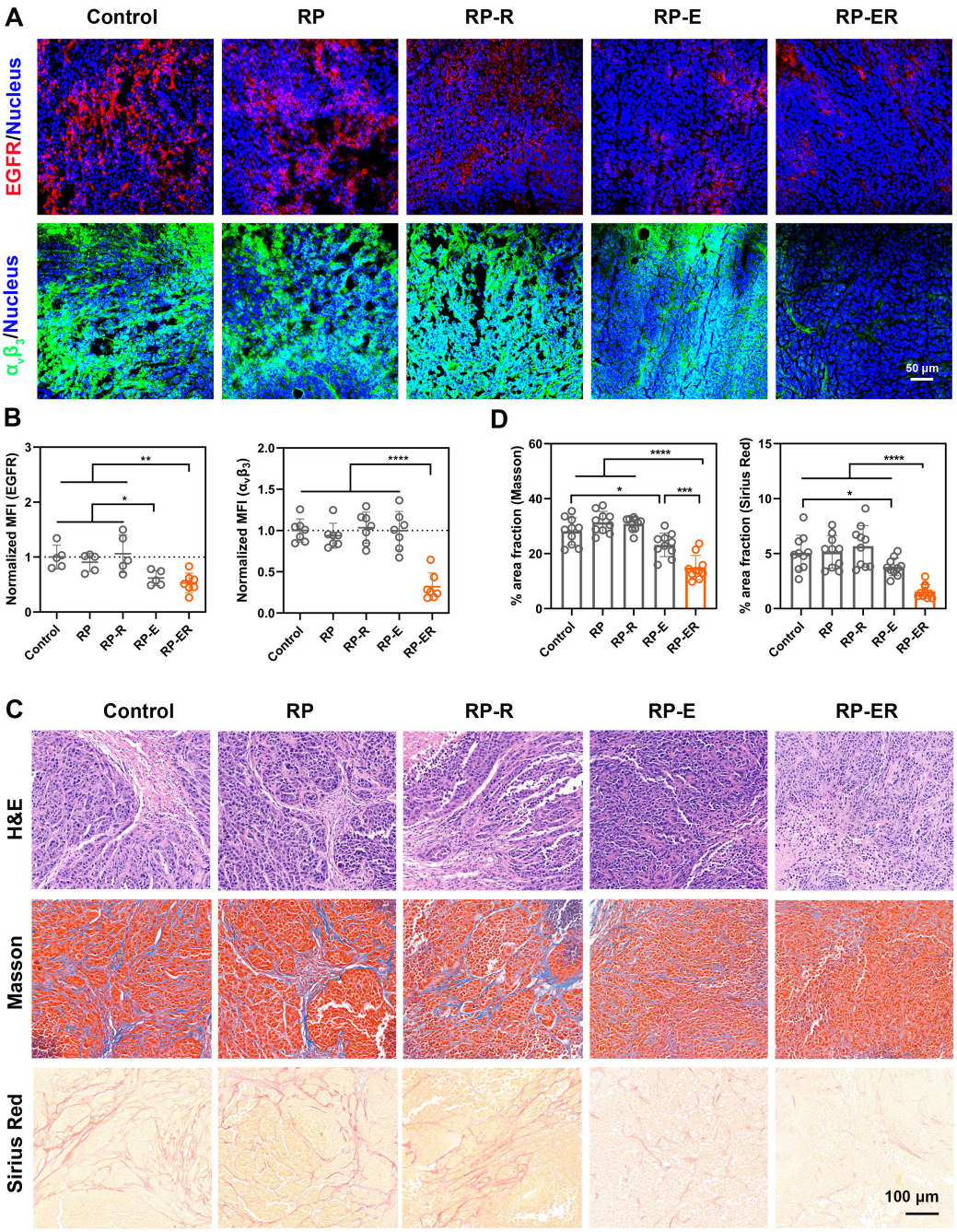

Figure S6. RP-ER reduces the expressions of EGFR, integrin $\alpha_v\beta_3$ and collagen I in HeLa tumors. A) The reduced expressions of EGFR and integrin $\alpha_v\beta_3$ were confirmed by immunofluorescence images of tumors slices. B) The MFIs were analyzed and normalized to that of free DOX. (n = 5–7). C, D) RP-ER regulates the expression of collagen I in HeLa tumors. The contents of collagen I were visualized (C) and semiquantitative analyzed (D) by hematoxylin and eosin (H&E) staining, Sirius Red staining and Masson staining. Data are presented in mean ± s.d. P values waere calculated using multiple t-tests. * $P < 0.05$, ** $P < 0.01$, **** $P < 0.0001$.

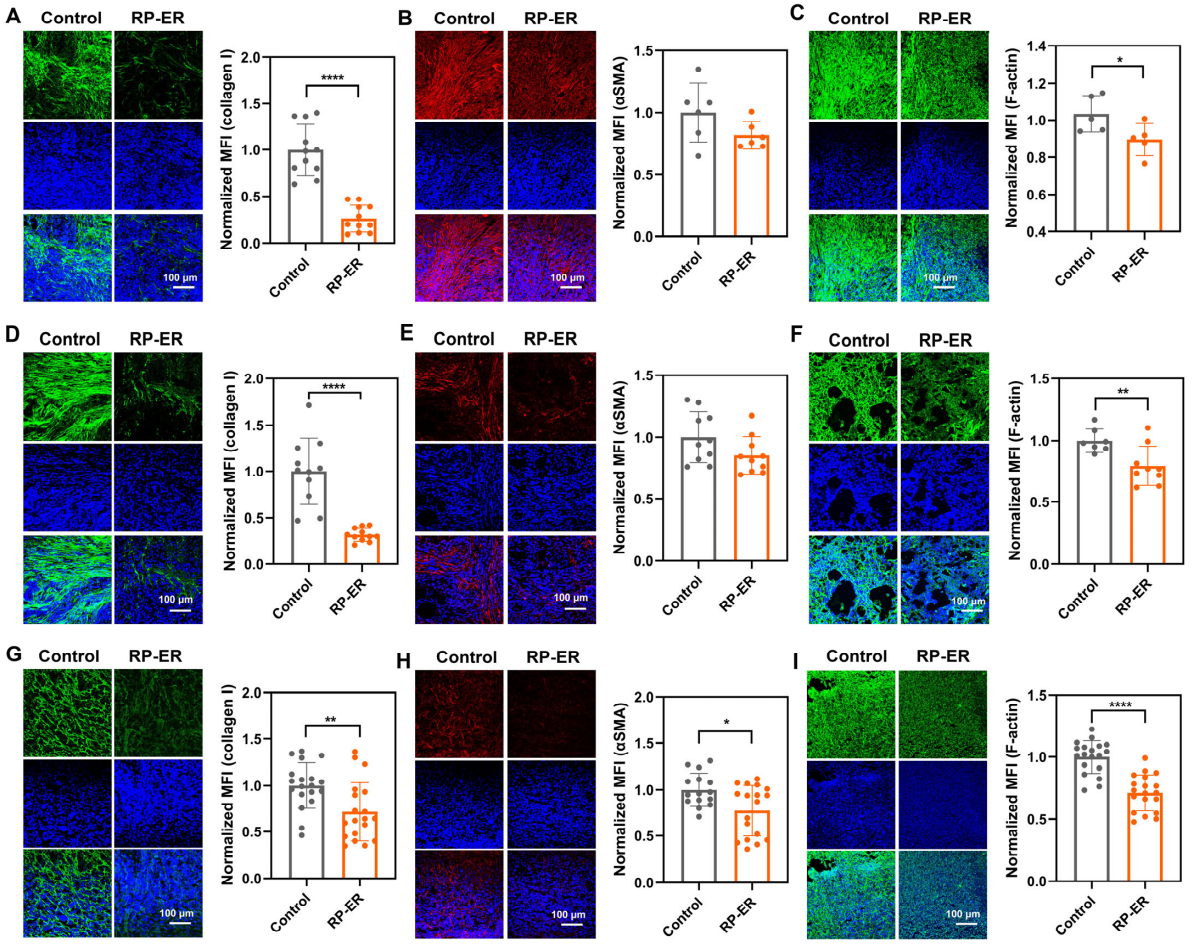

Figure S7. RP-ER regulates the expressions of collagen I, αSMA and F-actin in various tumors. A–C) RP-ER regulates the collagen I (A), αSMA (B) and F-actin (C) in MCF-7 tumors. (n = 5–11). D–F) RP-ER regulates the collagen I (D), αSMA (E) and F-actin (F) in A549 tumors. (n = 7–10). G–I) RP-ER regulates the collagen I (G), αSMA (H) and F-actin (I) in MDA-MB 231 tumors. (n = 18). Data are presented in mean ± s.d. P values were calculated using unpaired t-test. *P < 0.05, ** P < 0.01, **** P < 0.0001.

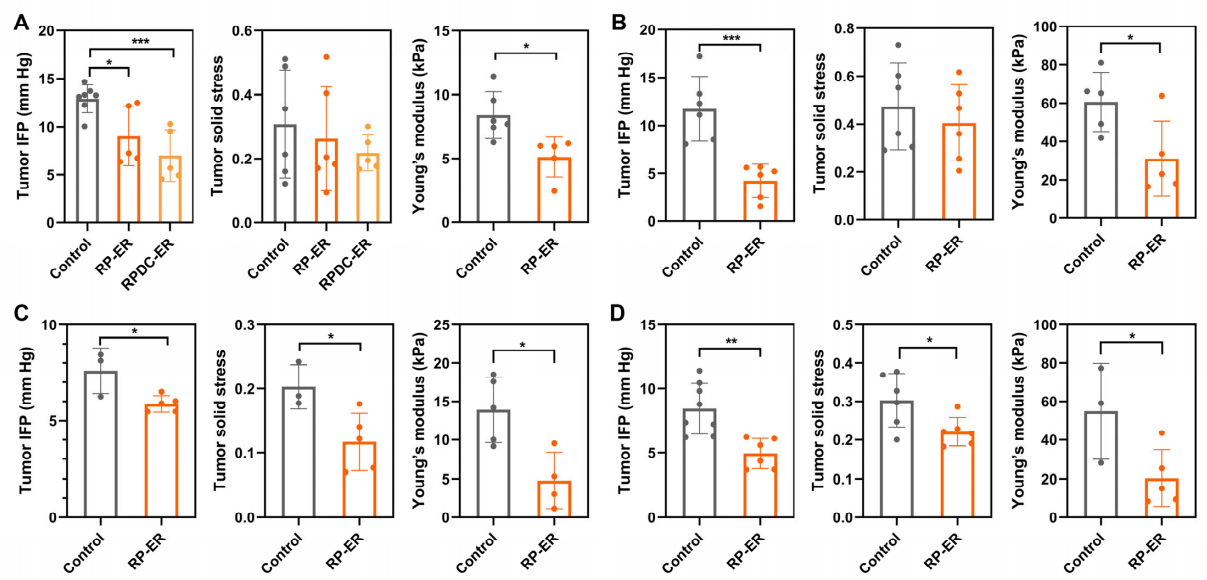

Figure S8. RP-ER changes the physical properties of various tumors.The IFP, solid stress and Young's modulus of MCF-7 tumors (A), A549 tumors (B), MDA-MB 231 tumors (C) and MIA PaCa-2 tumors (D) from tumor-bearing BALB/c nude mice treated with RP-ER or RPDC-ER (n = 3–8 tumors). Data are presented in mean ± sd. P values were calculated using unpaired t-test. *P < 0.05, *** P < 0.01.

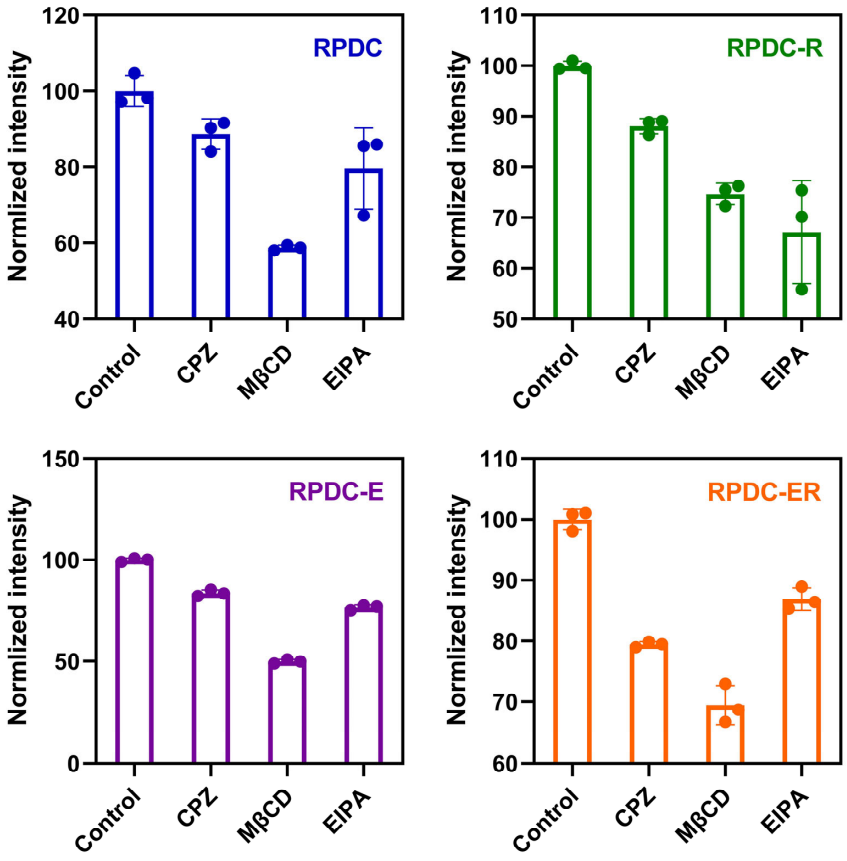

Figure S9. The endocytosis pathways of RPDCs in HeLa cells evaluated by a flow cytometry. Chlorpromazine (CPZ) (10 μM), Methyl-β-cyclodextrin (MβCD) (300 μM), 5-(N-ethyl-N-isopropyl) amiloride (EIPA) (100 μM) which are used as inhibitors of clathrin-mediated endocytosis, caveolae-mediated endocytosis, and micropinocytosis. (n = 3). Data are presented in mean ± s.d.

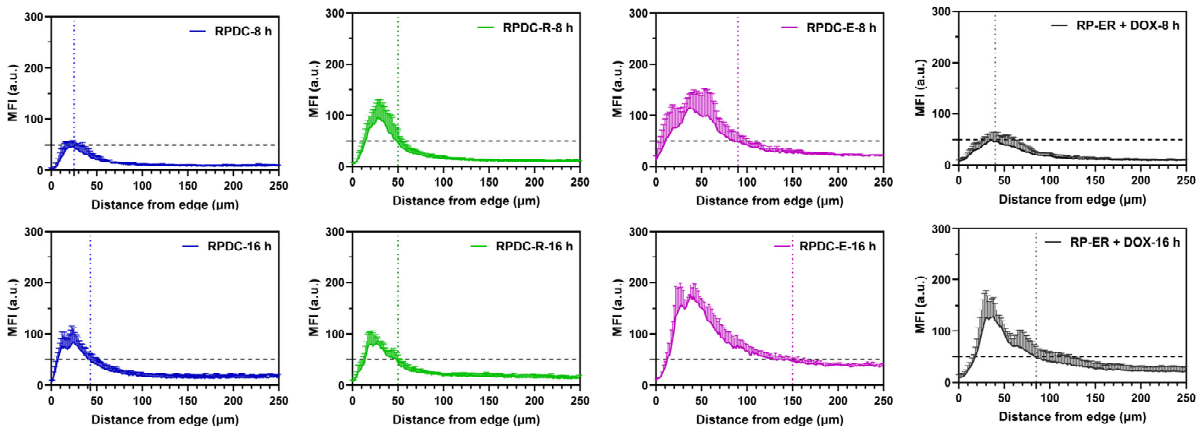

Figure S10. The radial distribution of different RPDCs based on MFIs in HeLa MCs for 8 h and 16 h. The fluorescence threshold for migration distance measurement is set as 50 and the migration distance for different agents are indicated as vertical bars with different color, respectively. (n = 3–7). Data are presented in mean ± s.d.

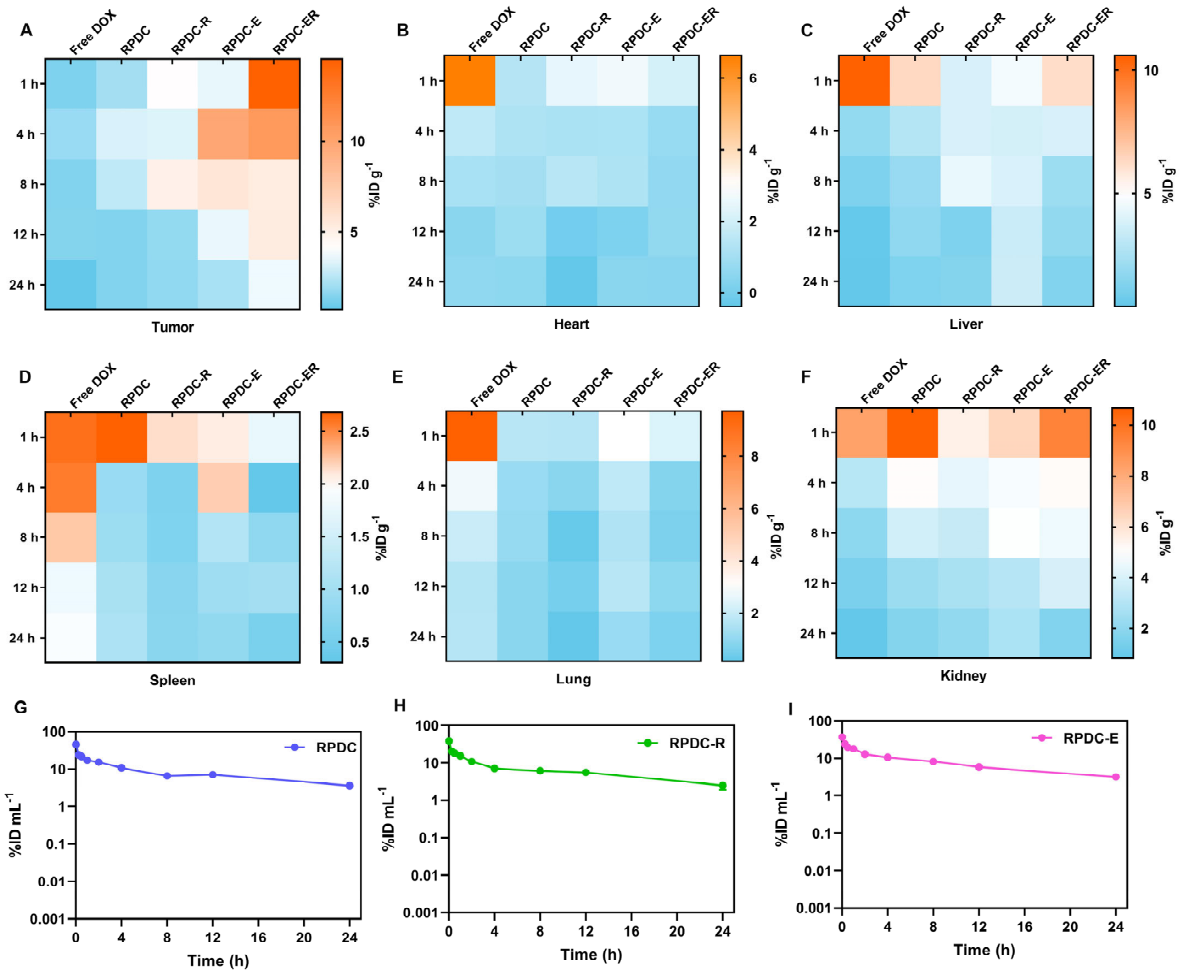

Figure S11. RPDC-ER improves the tissue biodistribution and pharmacokinetic of DOX. A) RPDC-ER significantly improves the DOX contents in HeLa tumors. Data are presented in mean average (n = 3). B–E) RPDC-ER significantly reduces the DOX content in heart (B), liver (C), spleen (D) and lung (E) in mice bearing HeLa tumors. Data are presented in mean average (n = 3). F) The DOX content in the kidney for RPDC-ER is similar to that of free DOX. Data are presented in mean average (n = 3). G–I) The pharmacokinetics of RPDC (G), RPDC-R (H) and RPDC-E (I) were evaluated in healthy ICR mice (n = 3). Data are presented in mean ± s.d.

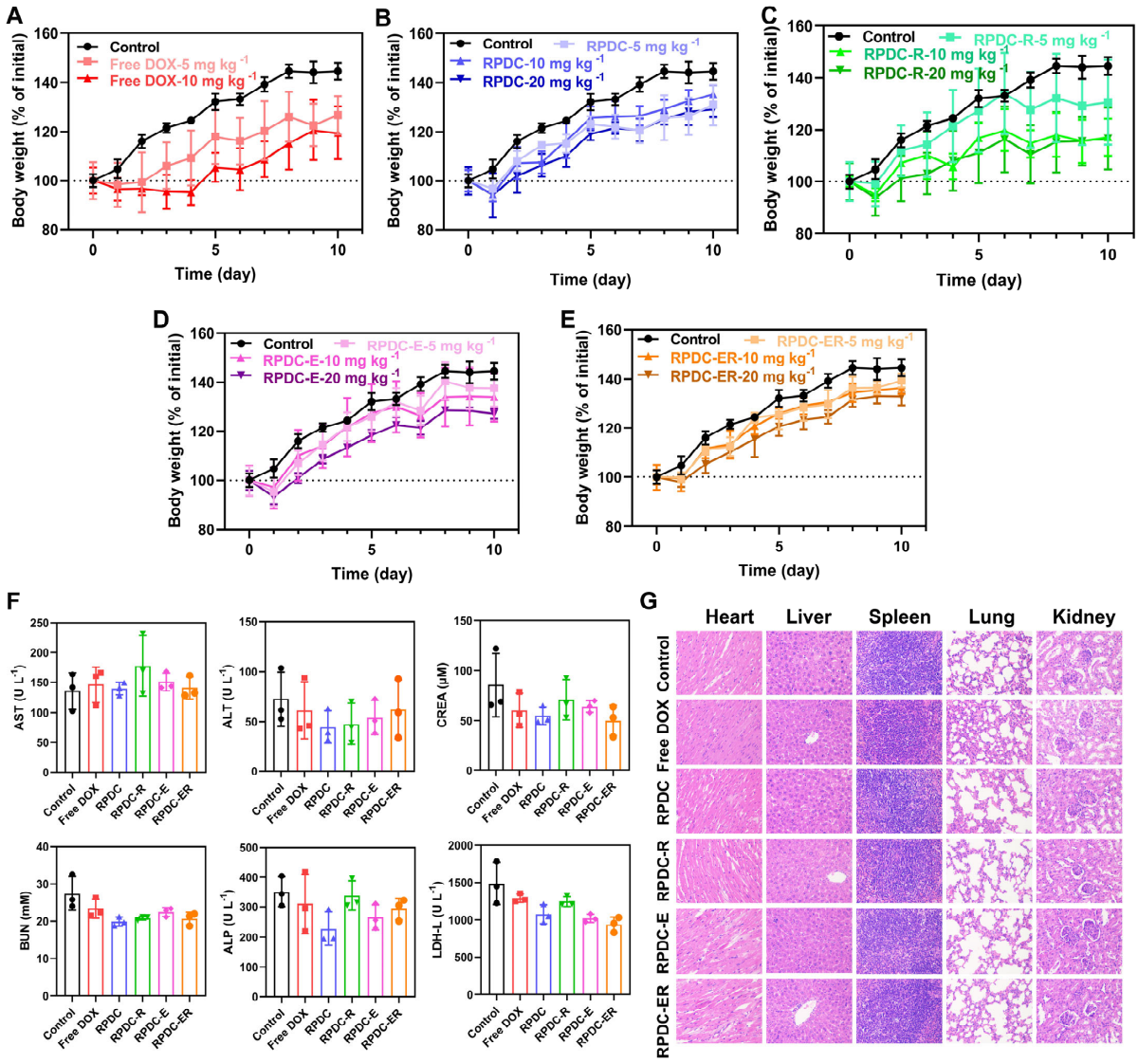

Figure S12. RPDC-ER exhibits a higher MTD. A–E) The body weights of healthy ICR male mice treated with PBS and different dosages of free DOX (A), RPDC (B), RPDC-R (C), RPDC-E (D), and RPDC-ER (E) (n = 3) were monitored and recorded each day for 10 days. Except mice treated with free DOX (10 mg kg^{-1}) showed a continuous body weight loss for four days, all mice in the other groups could recover one day after injection. The MTD of free DOX and other RPDCs were 5 and 20 mg kg^{-1}, respectively. Data are presented in mean ± s.d. F) The plasma biochemical parameters at the MTD of RPDCs are analyzed. No obvious toxicity was found for all groups. Data are presented in mean ± s.d. (n = 3). G) The organ tissue samples at the MTD of RPDCs are stained by hematoxylin and eosin (H&E) staining. No obvious damage was found for all groups.

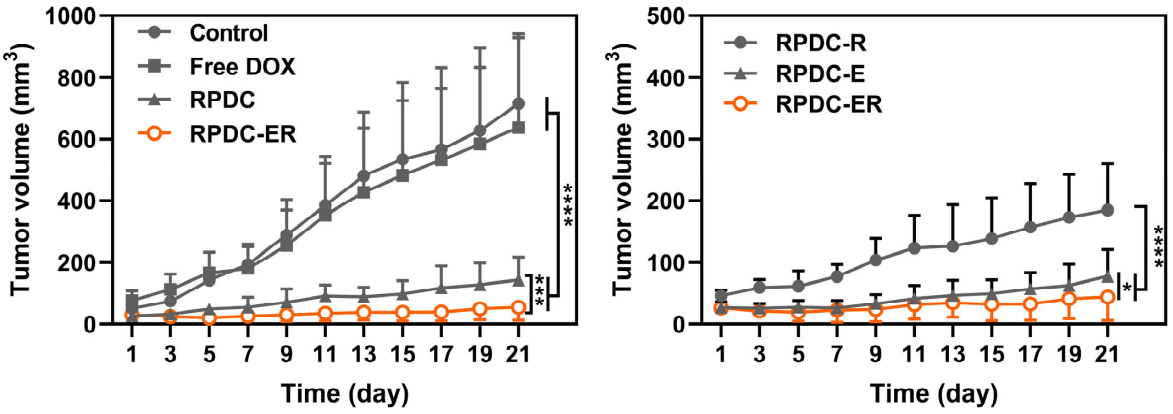

Figure S13. RPDC-ER exhibits a superior anticancer effect than other agents. HeLa tumors were treated with free DOX (5 mg kg^{-1}), RPDC (20 mg kg^{-1}, DOX eq.), RPDC-E (20 mg kg^{-1}, DOX eq.), RPDC-R (20 mg kg^{-1}, DOX eq.), RPDC-ER (20 mg kg^{-1}, DOX eq.) (n = 5). Data are presented in mean ± s.d. P values were calculated using multiple t-tests. * $P < 0.05$, *** $P < 0.001$, **** $P < 0.0001$.

References:

[1] W. Chen, S. Ji, X. Qian, Y. Zhang, C. Li, W. Wu, F. Wang, X. Jiang, *Polym. Chem.* **2017**, *8*, 2105-2114.

[2] D. E. Meyer, A. Chilkoti, *Nat. Biotech.* **1999**, *17*, 1112-1115.

[3] T. Kaneko, D. Willner, I. Monkovic, J. O. Knipe, G. R. Braslawsky, R. S. Greenfield, D. M. Vyas, *Bioconjugate Chem.* **1991**, *2*, 133-141.

[4] V. P. Chauhan, J. D. Martin, H. Liu, D. A. Lacorre, S. R. Jain, S. V. Kozin, T. Stylianopoulos, A. S. Mousa, X. Han, P. Adstamongkonkul, Z. Popović, P. Huang, M. G. Bawendi, Y. Boucher, R. K. Jain, *Nat. Commun.* **2013**, *4*, 2516.

[5] D. W. Huang, B. T. Sherman, R. A. Lempicki, *Nat. Protoc.* **2009**, *4*, 44-57.

[6] D. W. Huang, B. T. Sherman, R. A. Lempicki, *Nucleic Acids Res.* **2008**, *37*, 1-13.

[7] X. Wang, X. Zhen, J. Wang, J. Zhang, W. Wu, X. Jiang, *Biomaterials* **2013**, *34*, 4667-4679.

[8] S. Suh, A. Jo, M. A. Traore, Y. Zhan, S. L. Coutermarsh-Ott, V. M. Ringel-Scaia, I. C. Allen, R. M. Davis, B. Behkam, *Adv. Sci.* **2019**, *6*, 1801309.